Electronic Supplementary Material (ESI) for ChemComm.

Supporting Information

Infrared Spectroscopic and Theoretical Investigations of the novel Iridium Oxyfluorides

Yan Lu,[a] Robert Medel,[a] Guohai Deng,[a] Sebastian Riedel*[a]

[a] Y. Lu, Dr. R. Medel, Dr. G. H. Deng, Prof. Dr. S. Riedel
Freie Universität Berlin
Institut für Chemie und Biochemie–Anorganische Chemie
Fabeckstrasse 34/36, 14195 Berlin (Germany)
E-mail: s.riedel@fu-berlin.de

Contents

Experimental and computational details

The technique of matrix-isolation infrared (IR) spectroscopy and laser-ablation apparatus have been described in previous studies.[1,2,3] Matrix samples were prepared by co-deposition of laser-ablated iridium atoms with 0.02 % and 0.5 % OF_2 diluted in neon (99.999 %, Air Liquide) and argon (99.999 %, Sauerstoffwerk Friedrichshafen), respectively. The OF_2 was premixed with neon or argon in a custom-made stainless-steel mixing chamber.

The mixing chamber was connected to a self-made matrix chamber by a stainless-steel capillary. The gas mixture was condensed with laser-ablated iridium atoms onto a gold-plated mirror cooled to 5 K for neon and 12 K for argon using a closed-cycle helium cryostat (Sumitomo Heavy Industries, RDK-205D) inside the matrix chamber. For the laser-ablation, the 1064 nm fundamental of a Nd:YAG laser (Continuum, Minilite II, 10 Hz repetition rate, 55–60 mJ pulse^{-1}) was focused onto a rotating iridium metal target (∅ 10 mm) using a plano-convex lens (∅ 25.4 mm, focal length of 125.0 mm) through a hole in the cold mirror.

Preparation of $^{16/18}OF_2$ followed procedures described in the literature.[4] $^{16/18}OF_2$ was synthesized by the reaction of elemental fluorine and $^{16/18}OH_2$ dispersed in solid NaF.[4] Infrared spectra of the reaction products were recorded on a Bruker Vertex 80v spectrometer with a resolution of 0.5 cm^{-1} in the region 4000–450 cm^{-1} using a liquid-nitrogen-cooled mercury cadmium telluride (MCT) detector. Matrix samples were annealed at different temperatures, and the samples were subjected to photolysis using a mercury arc streetlamp (Osram HQL 250) with the outer globe removed ($\lambda > 220$ nm).

Density functional theory (DFT) calculations were performed using the Gaussian16 program package[5] employing the hybrid functional B3LYP[6] with the augmented triple-ζ basis sets aug-cc-pVTZ[7] for fluorine and oxygen and the aug-cc-pVTZ-PP[8] valence basis and associated scalar-relativistic pseudopotential (PP) for iridium. Subsequent structure optimizations as well as harmonic vibrational frequency analyses at the CCSD(T)[9](coupled-cluster singles-doubles with perturbational triples) level with aug-cc-pVTZ-PP basis sets were carried out in the spin unrestricted ROHF-UCCSD(T) open-shell coupled cluster formalism using default frozen core settings as implemented in the Molpro 2019 software package.[10]

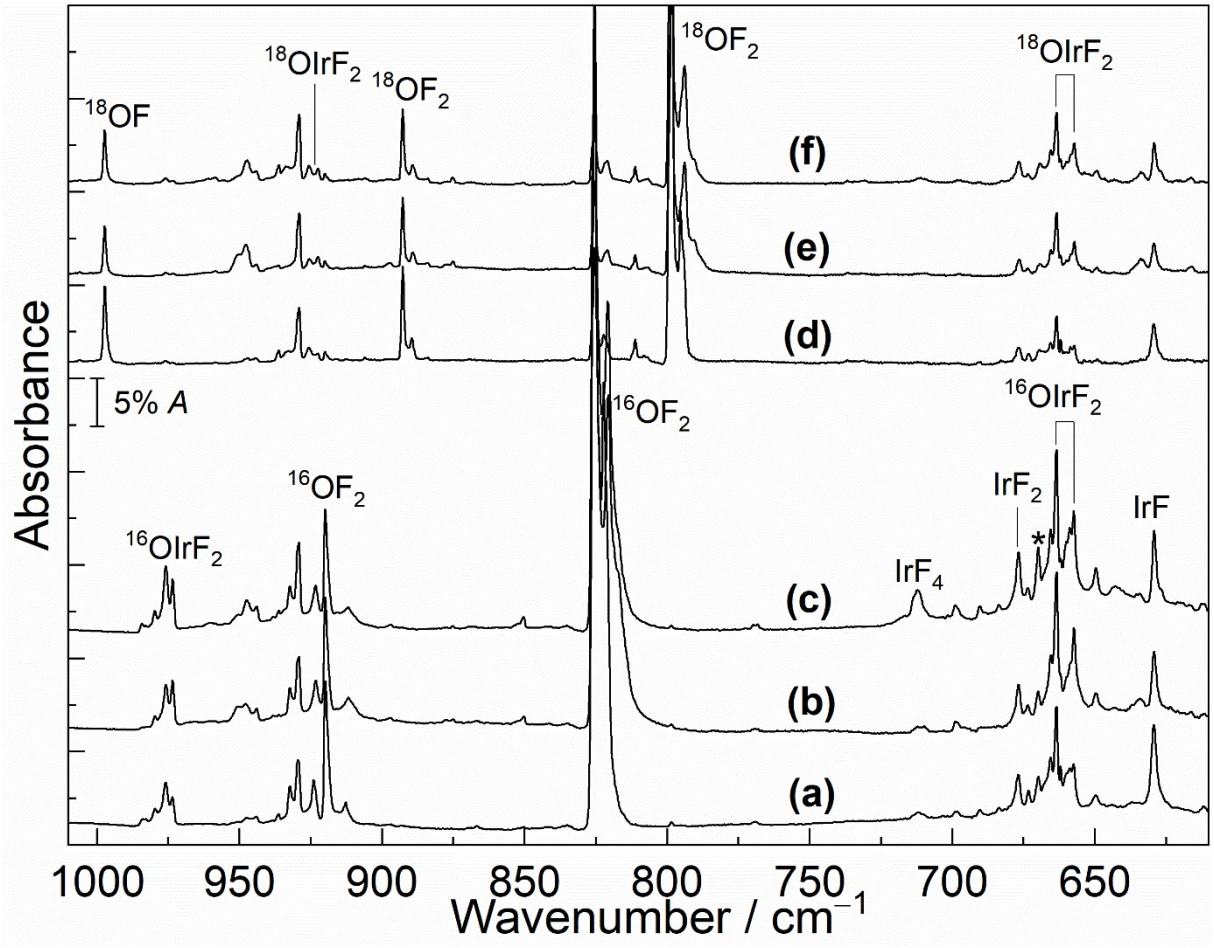

Figure S1. IR spectra in argon matrix at 12 K. (a) IR spectrum of reaction products of laser-ablated Ir atoms with 0.5% $^{16}OF_2$; (b) after annealing to 25 K; (c) after full-arc (> 220 nm) for 20 min. (d) IR spectrum of reaction products of laser-ablated Ir atoms with 0.5% $^{18}OF_2$; (e) after annealing to 25 K; (f) after full-arc (> 220 nm) for 20 min. The bands marked with asterisks are assigned to unknown impurities.

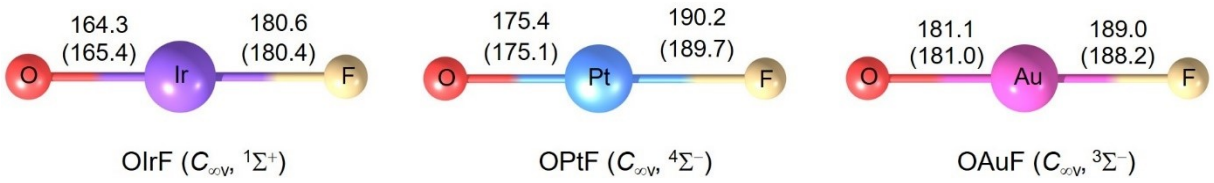

Figure S2. Optimized structures of OIrF, OPtF and OAuF in their ground states at B3LYP/aug-cc-pVTZ-PP level. Bond lengths in pm are shown. The CCSD(T) values are given in parentheses.

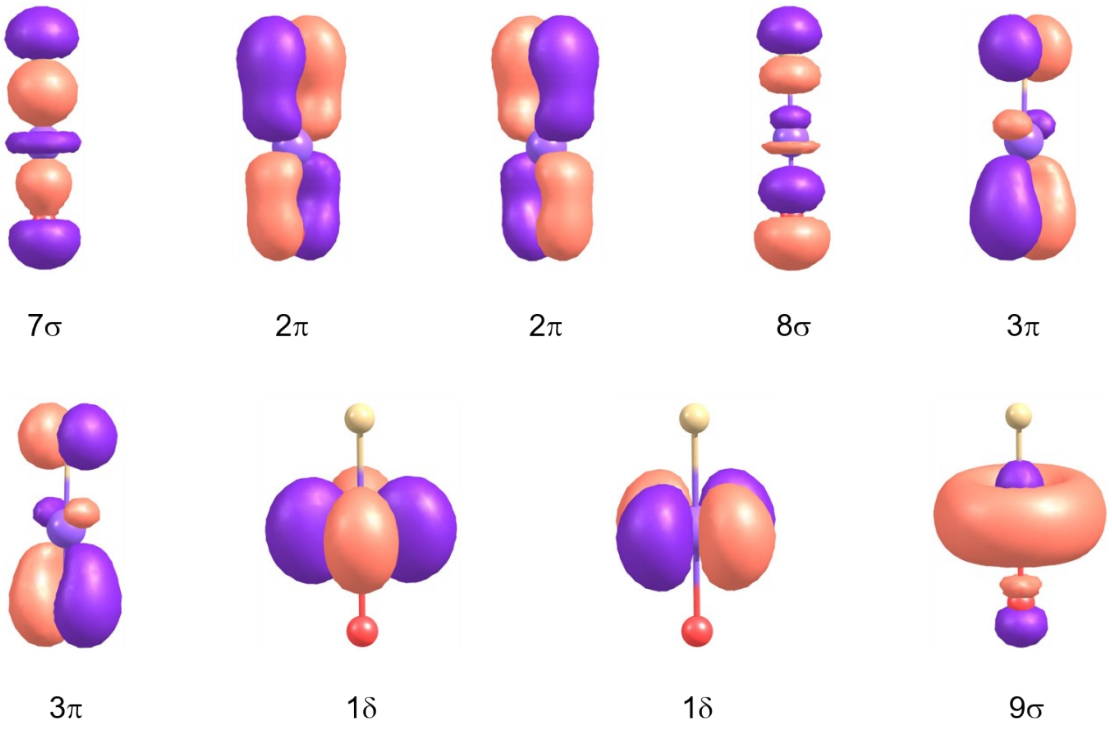

Figure S3. Molecular orbitals of OIrF computed at B3LYP/aug-cc-pVTZ-PP level.

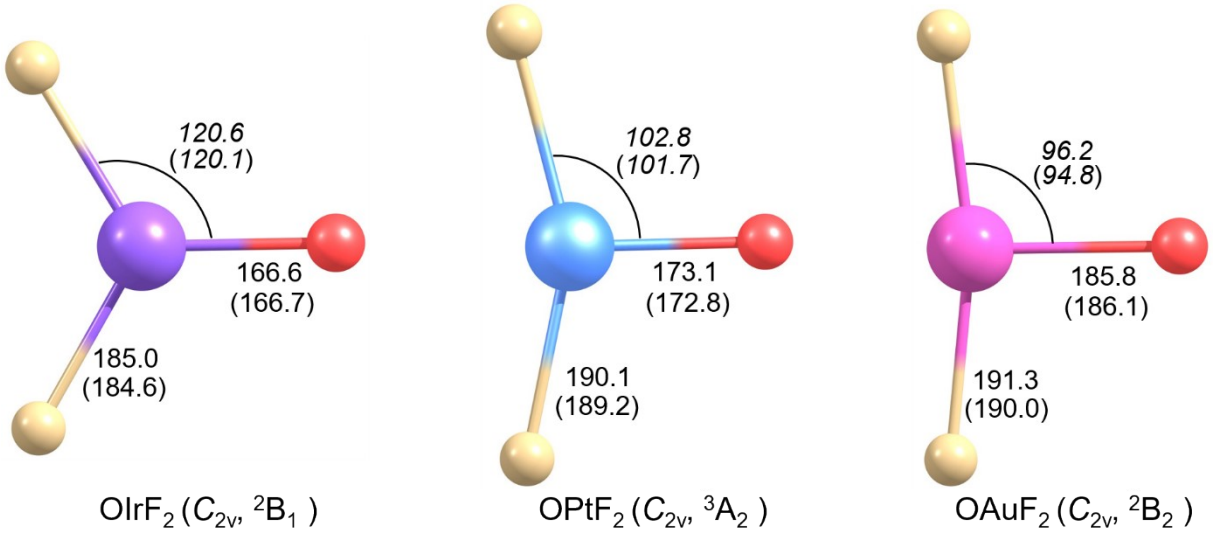

Figure S4. Optimized structures of $OIrF_2$, $OPtF_2$ and $OAuF_2$ in their ground states at B3LYP/aug-cc-pVTZ-PP level. Selected bond lengths in pm and angles in deg (in italics) are shown. The CCSD(T) values are given in parentheses.

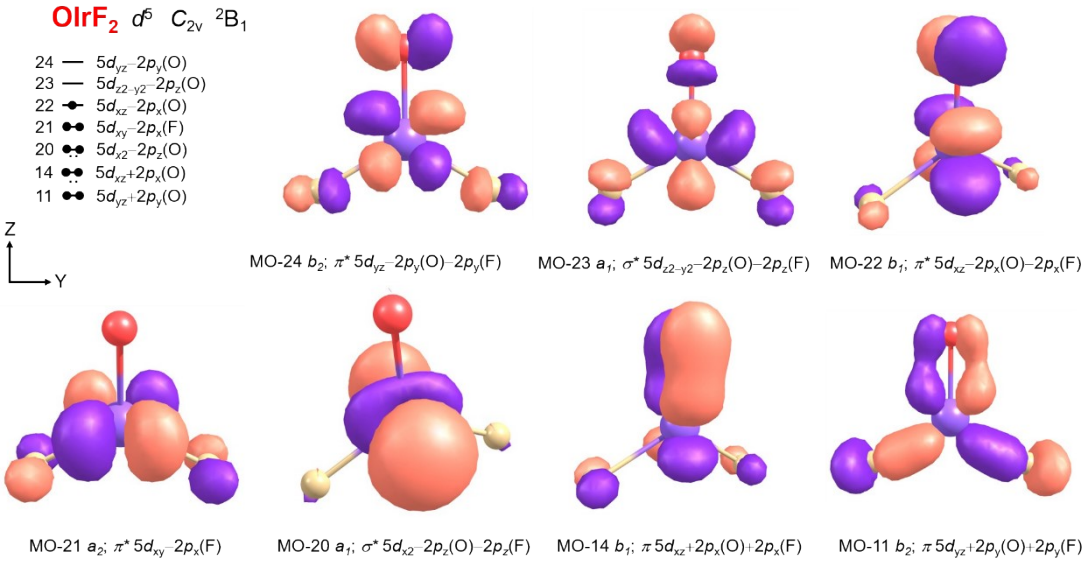

Figure S5. Selected molecular orbitals of $OIrF_2$ ($^2B_1$, C_{2v}). (B3LYP/AVTZ(-PP), Kohn-Sham orbitals with α spin; iso-surface = 0.09 electron a.u.$^{-3}$)

Table S1. Electronic states and electronic energy differences (kJ mol^{-1}) of $OIrF_2$ at scalar-relativistic pseudopotential levels.

Electronic state (Sym.)	CCSD(T)[a] $\Delta E + \Delta ZPE$	B3LYP[a] $\Delta E + \Delta ZPE$
$^2B_1$ (C_{2v})	0	0
$^4B_2$ (C_{2v})	97.4	81.9

[a]aug-cc-pVTZ-PP basis sets.

Table S2. Comparison of observed and computed vibrational frequencies (cm^{-1}) for $OIrF_2$.

	Ground state (Sym.)	Exp. Ne matrix	Ar matrix	Calc. (Int)[a] B3LYP	CCSD(T)	Modes
		984.1/980.7	976.0/973.6	1042.6 (64)	1033.1	ν(Ir–^{16}O)
$^{16}OIrF_2$	$^2B_1$ (C_{2v})	672.6	663.6	671.7 (115)	684.1	ν_{as}(Ir–F_2)
		666.8	657.5	670.5 (57)	682.8	ν_s(Ir–F_2)
		933.7/929.6	925.8/922.6	987.37 (58)	978.6	ν(Ir–^{18}O)
$^{18}OIrF_2$	$^2B_1$ (C_{2v})	672.6	663.6	671.7 (115)	684.1	ν_{as}(Ir–F_2)
		666.8	657.5	670.5 (57)	682.8	ν_s(Ir–F_2)

[a]aug-cc-pVTZ-PP basis sets. Intensities are shown in parentheses in km mol^{-1}. For the CCSD(T) calculations no intensities are available.

Table S3. Electronic states and electronic energy differences (kJ mol^{-1}) of FOIrF at scalar-relativistic pseudopotential levels.

Electronic state (Sym.)	CCSD(T)[a] $\Delta E + \Delta$ZPE	B3LYP[a] $\Delta E + \Delta$ZPE
^{2}A" (C_s)	16.5	–
^{4}A' (C_s)	1.2	4.9
^{4}A" (C_s)	0	0

[a]aug-cc-pVTZ-PP basis sets.

Table S4. Comparison of observed and computed vibrational frequencies (cm^{-1}) for FOIrF.

	Electronic state (Sym.)	Calc. (Int)[a] B3LYP	CCSD(T)	Exp. Ne matrix
		–	938.5	889.3
F^{16}OIrF	^{2}A" (C_s)	–	698.1	685.1
		–	464.4	–
		–	890.6	842.9
F^{18}OIrF	^{2}A" (C_s)	–	697.9	684.1
		–	446.1	–
		735.8 (65)	713.6	
F^{16}OIrF	^{4}A' (C_s)	621.4 (150)	625.9	
		489.6 (57)	524.2	
		704.5 (63)	741.7	
F^{16}OIrF	^{4}A" (C_s)	619.8 (162)	639.8	
		494.2 (98)	741.7	

[a]aug-cc-pVTZ-PP basis sets. Intensities are shown in parentheses in km mol^{-1}. For the CCSD(T) calculations no intensities are available.

Table S5. Electronic states, structural parameters (pm, deg), electronic energy differences (kJ mol^{-1}) of selected states of OIrF at scalar-relativistic pseudopotential levels.

Electronic state (Sym.)	CCSD(T)[a] Bond lengths [pm] O–Ir/Ir–F	Angle [°] O–Ir–F	ΔE + ΔZPE	B3LYP[a] Bond lengths [pm] O–Ir/Ir–F	Angle [°] O–Ir–F	ΔE + ΔZPE
$^1\Sigma^+$ ($C_{\infty v}$)	165.4/180.4	180.0	0	164.3/180.6	180.0	0
$^3\Sigma^-$ ($C_{\infty v}$)	173.9/193.9	180.0	190.3	–	–	–
$^3\Pi$ ($C_{\infty v}$)	169.8/186.6	180.0	72.6	169.0/186.9	180.0	54.7
$^5\Delta$ ($C_{\infty v}$)	175.8/192.9	180.0	134.4	176.3/193.3	180.0	111.9

[a]aug-cc-pVTZ-PP basis sets.

Table S6. Comparison of observed and computed vibrational frequencies (cm^{-1}) for OIrF.

	Ground state (Sym.)	Exp. Ne matrix	Calc. (Int)[a] B3LYP	CCSD(T)	Modes
^{16}OIrF	$^1\Sigma^+$ ($C_{\infty v}$)	– 732.2	1106.0 (76) 735.4 (95)	1053.4 741.7	ν(Ir–^{16}O) ν(Ir–F)
^{18}OIrF	$^1\Sigma^+$ ($C_{\infty v}$)	– 732.2	1047.5 (71) 735.1 (94)	998.0 741.4	ν(Ir–^{18}O) ν(Ir–F)

[a]aug-cc-pVTZ-PP basis sets. Intensities are shown in parentheses in km mol^{-1}. For the CCSD(T) calculations no intensities are available.

Table S7. Comparison of observed vibrational frequencies (in cm^{-1}) for OIrF, OPtF and OAuF.

Species	CCSD(T)[a] Calc.	Exp. Ne matrix	Modes
OIrF ($C_{\infty v}$, $^1\Sigma^+$)	1053.4	–	ν(Ir–O)
	741.7	732.2	ν(Ir–F)
OPtF ($C_{\infty v}$, $^4\Sigma^-$)[1]	848.3	–	ν(Pt–O)
	640.3	611.8	ν(Pt–F)
OAuF ($C_{\infty v}$, $^3\Sigma^-$)[2]	767.9	–	ν(Au–O)
	642.6	629.4	ν(Au–F)

[a]aug-cc-pVTZ-PP basis sets.

Table S8. Comparison of observed vibrational frequencies (in cm^{-1}) for $OIrF_2$, $OPtF_2$ and $OAuF_2$.

Species	CCSD(T)[a] Calc.	Exp. Ne matrix	Ar matrix	Modes
$OIrF_2$ (C_{2v}, $^2B_1$)	682.2	666.8	657.5	ν_s(Ir–F_2)
	684.1	672.6	663.6	ν_{as}(Ir–F_2)
	1033.1	980.7	973.6	ν(Ir–O)
$OPtF_2$ (C_{2v}, $^3A_2$)[1]	627.0	–	–	ν_s(Pt–F_2)
	652.2	650.2	635.2	ν_{as}(Pt–F_2)
	870.8	–	–	ν(Pt–O)
$OAuF_2$ (C_{2v}, $^2B_2$)[2]	616.0	–	–	ν(Au–O)
	621.4	–	–	ν_s(Au–F_2)
	659.2	655.3	634.6	ν_{as}(Au–F_2)

[a]aug-cc-pVTZ-PP basis sets. For the CCSD(T) calculations no intensities are available.

Table S9. Computed thermochemical stability of iridium oxyfluorides (298.15 K, kJ mol^{-1}) at B3LYP and CCSD(T) level.

Reaction	B3LYP[a]		CCSD(T)[a]	
	$\Delta E + \Delta$ZPE	$\Delta_r H$	$\Delta E + \Delta$ZPE	$\Delta_r H^b$
$Ir + OF \rightarrow OIrF$	−744.6	−746.8	−778.3	−780.8
$OIrF + F \rightarrow OIrF_2$	−332.6	−336.3	−307.7	−311.7
$Ir + OF_2 \rightarrow OIrF_2$	−924.5	−926.3	−929.7	−932.4
$FOIrF \rightarrow OIrF_2$	−	−	−389.0	−
$Ir + OF_2 \rightarrow FOIrF$	−	−	−540.7	−

[a]aug-cc-pVTZ-PP basis sets. [b]The enthalpies at CCSD(T) level were calculated by adding the enthalpy corrections (B3LYP) to electronic energy changes.

Calculated atomic coordinates (in Å) of species for optimized structures at B3LYP/aug-cc-pVTZ-PP level.

OIrF $^1\Sigma^+$ ($C_{\infty v}$):

Ir	0.00000000	0.00000000	0.03303700
O	0.00000000	0.00000000	1.67632500
F	0.00000000	0.00000000	-1.77271300

OIrF $^3\Pi$ ($C_{\infty v}$):

Ir	0.00000000	0.00000000	0.03518100
O	0.00000000	0.00000000	1.72473200
F	0.00000000	0.00000000	-1.83408400

OIrF $^5\Delta$ ($C_{\infty v}$):

Ir	0.00000000	0.00000000	0.03503900
O	0.00000000	0.00000000	1.79780500
F	0.00000000	0.00000000	-1.89782500

$OIrF_2$ $^2B_1$ (C_{2v}):

Ir	0.00000000	0.00000000	0.03532600
O	0.00000000	0.00000000	1.70111100
F	0.00000000	1.59208700	-0.90716600
F	0.00000000	-1.59208700	-0.90716600

$OIrF_2$ $^4B_2$ (C_{2v}):

Ir	0.00000000	0.00000000	0.09759100
O	0.00000000	0.00000000	1.81420900
F	0.00000000	1.33096300	-1.22379000
F	0.00000000	-1.33096300	-1.22379000

FOIrF $^4A''$ (C_s):

Ir	0.00000000	0.20313300	0.00000000
O	0.81361000	-1.44114500	0.00000000
F	-0.27832700	-2.49285500	0.00000000
F	-0.44488200	2.03596000	0.00000000

FOIrF $^4A'$ (C_s):

Ir	0.00000000	0.19608700	0.00000000
O	0.82568600	-1.46042700	0.00000000
F	-0.34059900	-2.42340800	0.00000000
F	-0.39334400	2.04393600	0.00000000

Calculated atomic coordinates (in Å) of species for optimized structures at CCSD(T)/aug-cc-pVTZ-PP level.

OIrF $^{1}\Sigma^{+}$ ($C_{\infty v}$):

Ir	0.0000000000	0.0000000000	0.0288126011
O	0.0000000000	0.0000000000	1.6830588551
F	0.0000000000	0.0000000000	-1.7752224562

OIrF $^{3}\Sigma^{-}$ ($C_{\infty v}$):

Ir	0.0000000000	0.0000000000	0.0454514358
O	0.0000000000	0.0000000000	1.7844925815
F	0.0000000000	0.0000000000	-1.8932950173

OIrF $^{3}\Pi$ ($C_{\infty v}$):

Ir	0.0000000000	0.0000000000	0.0348429644
O	0.0000000000	0.0000000000	1.7328641011
F	0.0000000000	0.0000000000	-1.8310580654

OIrF $^{5}\Delta$ ($C_{\infty v}$):

Ir	0.000000000	0.000000000	0.035492183
O	0.000000000	0.000000000	1.793250147
F	0.000000000	0.000000000	-1.893723380

OIrF$_2$ $^{2}B_1$ (C_{2v}):

Ir	0.0000000000	0.0000000000	0.0274677603
O	0.0000000000	0.0000000000	1.6944354444
F	0.0000000000	1.5967376484	-0.8998991024
F	0.0000000000	-1.5967376484	-0.8998991024

OIrF$_2$ $^{4}B_2$ (C_{2v}):

Ir	0.000000000	0.000000000	0.093466085
O	0.000000000	0.000000000	1.809982368

F	0.000000000	1.330190455	-1.219614246
F	0.000000000	-1.330190455	-1.219614246

FOIrF $^{2}A''$ (C_s):

Ir	-0.2413869467	-0.1209942502	0.0000000000
O	1.3923426250	-0.6448803225	0.0000000000
F	2.5960277687	0.6042594348	0.0000000000
F	-2.0510181670	0.2495297479	0.0000000000

FOIrF $^{4}A'$ (C_s):

Ir	0.0331075569	0.1872999277	0.0000000000
O	0.8600944827	-1.4832103073	0.0000000000
F	-0.3750426727	-2.3611201206	0.0000000000
F	-0.4264163669	2.0132185002	0.0000000000

FOIrF $^{4}A''$ (C_s):

Ir	0.033226368	0.186144793	0.000000000
O	0.858337570	-1.452030730	0.000000000
F	-0.323797835	-2.430704887	0.000000000
F	-0.477365103	2.001683823	0.000000000

References

1 L. Li, H. Beckers, T. Stüker, T. Lindič, T. Schlöder, D. Andrae and S. Riedel, *Inorg. Chem. Front.*, 2021, **8**, 1215.

2 L. Li, T. Stüker, S. Kieninger, D. Andrae, T. Schlöder, Y. Gong, L. Andrews, H. Beckers and S. Riedel, *Nat. Commun.*, 2018, **9**, 1267.

3 (*a*) R. Wei, Z. T. Fang, M. Vasiliu, D. A. Dixon, L. Andrews and Y. Gong, *Inorg. Chem.*, 2019, **58**, 9796; b) L. Andrews, X. Wang, Y. Gong, T. Schlöder, S. Riedel and M. J. Franger, *Angew. Chem. Int. Ed.*, 2012, **51**, 8235.

4 A. H. Borning and K. E. Pullen, *Inorg. Chem.*, 1969, **8**, 1791.

5 M. J. Frisch, G. W. Trucks, H. B. Schlegel, G. E. Scuseria, M. A. Robb, J. R. Cheeseman, G. Scalmani, V. Barone, G. A. Petersson, H. Nakatsuji, X. Li, M. Caricato, A. V. Marenich, J. Bloino, B. G. Janesko, R. Gomperts, B. Mennucci, H. P. Hratchian, J. V. Ortiz, A. F. Izmaylov, J. L. Sonnenberg, D. Williams-Young, F. Ding, F. Lipparini, F. Egidi, J. Goings, B. Peng, A. Petrone, T. Henderson, D. Ranasinghe, V. G. Zakrzewski, J. Gao, N. Rega, G. Zheng, W. Liang, M. Hada, M. Ehara, K. Toyota, R. Fukuda, J. Hasegawa, M. Ishida, T. Nakajima, Y. Honda, O. Kitao, H. Nakai, T. Vreven, K. Throssell, J. A. Montgomery, Jr., J. E. Peralta, F. Ogliaro, M. J. Bearpark, J. J. Heyd, E. N. Brothers, K. N. Kudin, V. N. Staroverov, T. A. Keith, R. Kobayashi, J. Normand, K. Raghavachari, A. P. Rendell, J. C. Burant, S. S. Iyengar, J. Tomasi, M. Cossi, J. M. Millam, M. Klene, C. Adamo, R. Cammi, J. W. Ochterski, R. L. Martin, K. Morokuma, O. Farkas, J. B. Foresman, and D. J. Fox, *Gaussian 16*, Gaussian, Inc., Wallingford CT, 2016.

6 (*a*) P. J. Stephens, F. J. Devlin, C. F. Chabalowski and M. J. Frisch, *J. Phys. Chem.*, 1994, **98**, 11623; (*b*) A. D. Becke, *J. Chem. Phys.*, 1993, **98**, 5648; (*c*) C. Lee, W. Yang and R. G. Parr, *Phys. Rev. B*, 1988, **37**, 785; (*d*) S. H. Vosko, L. Wilk and M. Nusair, *Can. J. Phys.*, 1980, **58**, 1200.

7 R. A. Kendall, T. H. Dunning and R. J. Harrison, *J. Chem. Phys.*, 1992, **96**, 6796.

8 (*a*) D. Figgen, K. A. Peterson, M. Dolg and H. Stoll, *J. Chem. Phys.*, 2009, **130**, 164108; (*b*) K. A. Peterson, D. Figgen, M. Dolg and H. Stoll, *J. Chem. Phys.*, 2007, **126**, 124101.

9 (*a*) K. Raghavachari, G. W. Trucks, J. A. Pople and M. Head-Gordon, *Chem. Phys. Lett.*, 1989, **157**, 479; (*b*) G. D. Purvis and R. J. Bartlett, *J. Chem. Phys.*, 1982, **76**, 1910.

10 H. -J. Werner, P. J. Knowles, G. Knizia, F. R. Manby, M. Schütz, P. Celani, W. Györffy, D. Kats, T. Korona, R. Lindh, A. Mitrushenkov, G. Rauhut, K. R. Shamasundar, T. B. Adler, R. D. Amos, S. J. Bennie, A. Bernhardsson, A. Berning, D. L. Cooper, M. J. O. Deegan, A. J. Dobbyn, F. Eckert, E. Goll, C. Hampel, A. Hesselmann, G. Hetzer, T. Hrenar, G. Jansen, C. Köppl, S. J. R. Lee, Y. Liu, A. W. Lloyd, Q. Ma, R. A. Mata, A. J. May, S. J. McNicholas, W. Meyer, T. F. Miller III, M. E. Mura, A. Nicklass, D. P. O'Neill, P. Palmieri, D. Peng, K. Pflüger, R. Pitzer, M. Reiher, T. Shiozaki, H. Stoll, A. J. Stone, R. Tarroni, T. Thorsteinsson, M. Wang, M. Welborn, *MOLPRO, version 2019.2, a package of ab initio programs*.